

# The Dependence of Globular Cluster Number on Density for Abell Cluster Central Galaxies<sup>1</sup>

John P. Blakeslee<sup>2</sup>

Department of Physics, Massachusetts Institute of Technology, Cambridge, MA 02139

## ABSTRACT

A study of the globular cluster systems of 23 brightest, or central, galaxies in 19 Abell clusters has recently been completed (Blakeslee 1997). This letter presents some of the newly discovered correlations of the globular cluster specific frequency  $S_N$  in these galaxies with other galaxy and cluster properties and puts forth an interpretation of these results.  $S_N$  is found to correlate strongly with measures of the cluster density, such as the velocity dispersion of the cluster galaxies and the cluster X-ray temperature and luminosity (especially “local” X-ray luminosity). Within a cluster, galaxies at smaller projected distances from the X-ray center are found to have higher values of  $S_N$ . Taken together, the scaling of  $S_N$  with cluster density and the relative constancy of central galaxy luminosity suggest a scenario in which globular clusters form in proportionate numbers to the available mass, but galaxy luminosity “saturates” at a maximum threshold, resulting in higher  $S_N$  values for central galaxies in denser clusters as well as the suitability of these galaxies as “standard candles.” Thus, these galaxies do not have too many globular clusters for their luminosity, they are underluminous for their number of globular clusters.

*Subject headings:* galaxies: clusters: general — galaxies: elliptical and lenticular, cD — galaxies: star clusters — globular clusters: general

---

<sup>1</sup>Observations conducted at the Michigan-Dartmouth-MIT Observatory

<sup>2</sup>Current address: Palomar Observatory, California Institute of Technology, Mail Stop 105-24, Pasadena, CA 91125; jpb@astro.caltech.edu

## 1. Introduction

The number of globular clusters (GCs) per unit galaxy luminosity is known as the globular cluster “specific frequency”  $S_N$  (Harris & van den Bergh 1981). Some central dominant galaxies in clusters, such as M87 in Virgo, have huge GC populations, or systems (GCSs), even when their large luminosities are taken into consideration (see Harris 1991 and references therein). These galaxies are often called “high- $S_N$  systems” and sometimes described as having “excess” GC populations. Although the high- $S_N$  systems are usually viewed as a special class of object, whether they represent the upper end of a continuum or are truly distinct has not previously been established. Because of the rarity of these objects, there have been few observational constraints on theories of their formation.

In an effort to address this situation, Blakeslee & Tonry (1995) developed an analysis technique for studying GCSs at relatively large distances and used it to study the GCSs of the two giant central galaxies in the Coma cluster. The technique is adapted from the methods used in the surface brightness fluctuations distance survey (Tonry et al. 1997), with the basic idea being that the portion of the GCS below the limit of direct photometric detection still produces a measurable signal in the power spectrum of the galaxy image. Wing et al. (1995) independently used the same approach to study the M87 GCS.

We have applied this technique to study a large, complete sample of brightest galaxies in Abell clusters. Our intent was to learn which central galaxies are high- $S_N$  systems, which are not, and why. A complete description of all aspects of this project is given by Blakeslee (1997; hereafter B97). Most of the details and the results will be published in a forthcoming paper (Blakeslee, Tonry, & Metzger 1997; hereafter BTM). The present Letter summarizes the observational sample, presents some of the most provocative new correlations of central galaxy  $S_N$  with properties of the galaxy clusters, and offers a new interpretation of the high  $S_N$  galaxies. Unlike other models which have attempted to explain  $S_N$  variations in terms of GC formation efficiency, this interpretation sees the relative insensitivity of galaxy luminosity to environmental density as the main culprit behind the large variations in  $S_N$ .

## 2. The Data

The details of the sample selection, observations, and reductions are given elsewhere (B97) and will be discussed again by BTM. Here we only summarize these aspects of the project and concentrate on the trends of  $S_N$  with cluster properties for our sample of Abell cluster central galaxies.

The sample of galaxies studied here was selected from the Lauer & Postman (1994;

hereafter LP) survey of 119 brightest cluster galaxies (BCGs) in Abell clusters and supplemented by the partial list of second brightest, or ranked, cluster galaxies (SRGs) from Postman & Lauer (1995; hereafter PL). Specifically, the current sample includes all early-type BCGs in northern Abell clusters with  $cz < 10000 \text{ km s}^{-1}$ , absolute  $R$ -band metric magnitude  $M_R < -22.0 + 5 \log h_{75}$ , and galactic latitude  $|b| > 15^\circ$ . (The early-type and  $M_R$  criteria exclude just two Abell clusters each.) It also includes three second brightest galaxies, and one third brightest, because these galaxies were similar to the respective BCGs in luminosity and extent. The final sample then comprises 23 galaxies in 19 Abell clusters, including the two Coma galaxies studied by Blakeslee & Tonry (1995). The observations were conducted with the 2.4 m telescope at the Michigan-Dartmouth-MIT Observatory on Kitt Peak over the course of several observing runs. Total integration times on the sample galaxies ranged from just over 1 hr to nearly 6.5 hr, determined by the prevailing image quality, the galaxy distance, and the available time.

The reduction process for the images is basically the same as that described by Blakeslee & Tonry 1995. For each final galaxy image, we model and subtract the galaxy light, then run the automatic photometry program DoPhot (Schechter et al. 1993). After correcting for the presence of dwarf and background galaxies in the object counts, we arrive at an estimate of the total number of GCs brighter than the cutoff magnitude  $m_c$  (determined by artificial star tests). We then remove all objects brighter than  $m_c$  from the image and measure the power spectrum of what remains. In order to estimate the total number of GCs fainter than  $m_c$ , the power spectrum measurement must be corrected for background galaxies and stellar SBF; the contribution from possible faint dwarf galaxies in the halo of the BCG is negligible at these magnitudes (see BTM).

The DoPhot object counts and power spectrum measurement each provide an estimate of the total number of GCs, given a luminosity function (GCLF); dividing the total number of GCs by the galaxy luminosity yields  $S_N$ . We assume the M87 GCLF (Whitmore et al. 1995) and calculate a weighted average of the two values of  $S_N$  derived for each galaxy, one from the counts and the other from the power spectrum. The agreement between the two separate measurements indicates that the use of the M87 GCLF is justified (B97; BTM).

### 3. Specific Frequencies

#### 3.1. Results for Individual Galaxies

Table 1 lists the values of  $S_N$  for each of the program galaxies, identified by the Abell cluster number and the luminosity rank in the cluster. In order to avoid uncertain

extrapolations and redshift biases in  $S_N$ , the table gives “metric  $S_N$ ” values, calculated within the same physical radius of  $32 h^{-1}$  kpc of the center of each galaxy, excluding the unusable galaxy center. The metric radius of  $32 h^{-1}$  kpc was chosen because it corresponds to the limit of the image for the nearest of the sample galaxies (roughly 500 pix, or  $2'.3$ , in the  $1024^2$  images). In calculating  $S_N$ , we adopted a zero point for the galaxy luminosities based on a Virgo distance of 16 Mpc. The distance zero point is unimportant, however, as any observed trends will be independent of it.

The tabulated  $S_N$  uncertainties include contributions from measurement error, relative distance error due to an assumed one-dimensional rms peculiar velocity of  $400 \text{ km s}^{-1}$  for the galaxy clusters in the CMB frame, and intrinsic dispersions of  $\pm 0.20$  and  $\pm 0.05$  mag for the mean and width of the GCLF, respectively (Harris 1996; B97). Uncertainties due to the distance, velocity, or GCLF calibrations, which could systematically change all the values by perhaps 20%, are not included. The  $S_N$  values shown for A1656-1 (NGC 4889) and A1656-2 (NGC 4874) differ from the global values reported by Blakeslee & Tonry (1995) primarily due to the faulty RC2 photometry used in that study, but also because the earlier values were calculated within a larger radius.

As evident from the table, there is no separation of “normal” and “anomalous”  $S_N$  classes in this sample of Abell cluster central galaxies.  $S_N$  varies uniformly from  $\sim 3$  to  $\sim 9$ . In the three clusters represented by more than one member, the SRGs all have the higher  $S_N$  values, though the difference is not significant in the case of A539. This is a result of selection. The SRGs were included in this sample because they all appear to dominate their clusters at least as much as the actual BCGs selected by LP. Moreover, these galaxies all have more extended profiles and are closer to the cluster X-ray centers than their respective BCGs. The relevance of these points will be clarified below.

### 3.2. $S_N$ and Cluster Density

A major result of this project is the strong dependence found for central galaxy  $S_N$  on cluster density. Figure 1 shows the  $S_N$  values from Table 1 plotted against the Abell cluster velocity dispersions, from Beers et al. (1991), Girardi et al. (1993), Scodreggio et al. (1995), Struble & Rood (1991), and Zabludoff et al. (1993). For the three clusters with multiple members, the more central galaxies (judged by the cluster X-ray center) are the ones shown as the filled symbols, and the less central ones are shown as open circles, even though three of these were chosen as BCGs by LP. The figure clearly indicates that central galaxies in higher dispersion clusters, and thus at the centers of deeper potential wells, have significantly more GCs per unit luminosity than those in lower dispersion clusters. (The

significance of the correlation is near 1.0 for the filled symbols.)

Perhaps the best measure of the depth of the cluster potential is the temperature  $T_X$  of the intracluster X-ray emitting gas. However, relatively few of these clusters have had this quantity directly measured, so we use instead the cluster X-ray luminosity  $L_X$ . Figure 2 plots  $S_N$  against the logarithm of  $L_X$  measured in the 0.5–4.5 keV band from Jones & Forman (1997). While previous investigations found no correlations of  $S_N$  with X-ray properties (Harris et al. 1995; West et al. 1995), our larger, more homogeneous data set clearly shows that there is a correlation.

Recently, West et al. (1995) have discussed the possibility of a population of “intracluster globular clusters” (IGCs) which belong to a galaxy cluster as a whole, not to individual galaxies. The hypothetical IGCs trace the cluster mass profile; assuming hydrostatic equilibrium and an isothermal potential implies that their surface density will be proportional to  $T_X/(1 + r^2/r_c^2)$ , where  $r$  is the projected distance of the galaxy from the cluster X-ray center, and  $r_c$  is the core radius. In this scenario, a large galaxy near the center of a cluster will appear to have an elevated value of  $S_N$  because some of these IGCs will have become associated with it.

Guided by West et al., we plot  $S_N$  against  $L_X/(1 + r^2/r_c^2)$ , the “local X-ray luminosity”, in Figure 3. (This differs from the corresponding figure in B97 because a calculational error in that work resulted in the use of core radii that were systematically too large.) The scatter in the relation decreases by  $\sim 5\%$  with this radial weighting. However, for reasons discussed by B97, i.e., the theoretical problems in producing the IGC population and the relatively low velocity dispersion observed in the very high  $S_N$  GCS of M87, we prefer to think of all the GCs as being bound to the host galaxy. The improvement of the  $S_N$ – $L_X$  correlation with the radial weighting would then be related to environmental effects having to do with the relative dominance of the galaxy in the cluster potential.

The correlations shown here between the  $S_N$  value of the central bright galaxy in the cluster and measures of the depth of the cluster potential might be explained in a number of ways. For instance: (1) the efficiency of GC formation for galaxies in denser regions may have been higher, for whatever reason; (2) central galaxies in clusters may strip GCs over time from other cluster members; or (3) the number of GCs scales with the cluster mass, but central galaxy luminosity does not, resulting in higher values of  $S_N$  and the observed independence of BCG luminosity on cluster properties. This final possibility has the aesthetic advantage of combining two separate problems into one. This issue is discussed more in the following section.

## 4. Discussion

We have established that central cluster galaxy  $S_N$  scales with measures of Abell cluster size, in particular, velocity dispersion and X-ray properties. (B97 shows that it also correlates to a lesser degree with cluster richness, but not morphology.) We have also found that for clusters with multiple galaxies in this sample, the one with the higher  $S_N$  value is the one which was closer to the cluster X-ray center.

So far, we have not discussed correlations of  $S_N$  with properties of the host galaxy. The obvious property to choose is galaxy luminosity, but due to the relatively small variation in this quantity among BCGs (PL and references therein), any correlation of  $S_N$  with luminosity for this sample of galaxies is marginal (B97; see also Harris 1991). A better, though still comparatively weak, correlation is found with galaxy extent, as measured, for example, by the profile “structure parameter”  $\alpha$ , the logarithmic slope of the integrated galaxy luminosity evaluated at  $r = 10 h^{-1} \text{ kpc}$ . It should be recognized, however, that  $\alpha$  was first introduced by Hoessel (1980) in order to remove the weak richness dependence of the BCG “standard candle” distance indicator. Figure 4 illustrates this situation, with  $\alpha$  plotted against  $S_N$  in the top panel and against cluster velocity dispersion in the lower panel. The two correlations are of similar significance levels; both have much greater scatter than the relation between  $S_N$  and cluster density or X-ray luminosity.

B97 has advanced a unified view of the observed  $S_N$  variations and the “standard candle” aspect of BCGs. In this view, GCs form early and in proportion to the local mass density, thus the observed excellent correlations of their number with cluster velocity dispersion and X-ray properties. (There is no need to invoke dark matter biasing.) On the other hand, the luminosity of the central galaxy saturates, speculatively due to the process of cluster formation itself. The collapse and subsequent virialization of a cluster from many smaller, irregular groups of galaxies might well disturb the gas in a large, centrally located galaxy in such a way as to halt subsequent star formation, adding to the hot intracluster gas and perhaps leaving as its signature the characteristic shallow profiles of these galaxies (i.e., the observed correlation with  $\alpha$ ).

Although the scenario remains uncertain, it is clear that central galaxy GC number depends on cluster scale, and can therefore itself be considered a cluster property, while the galaxy luminosity does not. Our proposal is that the same situation gives rise to both the high values of  $S_N$  measured for some galaxies, and the suitability of BCGs as “standard candles.” In light of these results, we suggest that the proper galaxy to use for measuring distances based on the  $L_m$ - $\alpha$  indicator is the bright extended galaxy closest to the cluster center; we predict that this galaxy will also be the one with the highest  $S_N$ .

I thank my thesis advisor John Tonry for insight-filled discussions. This research was supported by NSF grant AST94-01519 and by a Caltech Fairchild Fellowship.

## REFERENCES

- Beers, T. C., Forman, W., Huchra, J. P., Jones, C., & Gebhardt, K. 1991, *AJ*, 102, 1581
- Blakeslee, J. P. 1997, PhD Thesis, Massachusetts Institute of Technology (B97)
- Blakeslee, J. P. & Tonry, J. L. 1995, *ApJ*, 442, 579
- Blakeslee, J. P., Tonry, J. L. & Metzger, M. R. 1997, *AJ*, submitted (BTM)
- Girardi, M., Biviano, A., Giuricin, G., Mardirossian, F., & Mezzetti, M. 1993, *ApJ*, 404, 38
- Harris, W. E. 1991, *ARA&A*, 29, 543
- Harris, W. E. 1996, poster presented May 1996, STScI Symposium on the Distance Scale
- Harris, W. E., Pritchet, C. J., & McClure, R. D. 1995, *ApJ*, 441, 120
- Harris, W. E. & van den Bergh, S. 1981, *AJ*, 86, 1627
- Hoessel, J. G. 1980, *ApJ*, 241, 493
- Jones, C. & Forman, W. 1997, in preparation
- Lauer, T. R. & Postman, M. 1994, *ApJ*, 425, 418
- Postman, M. & Lauer, T. R. 1995, *ApJ*, 440, 28
- Schechter, P. L., Mateo, M., & Saha A. 1993, *PASP*, 105, 1342
- Scodeggio, M., Solanes, J. M., Giovanelli, R., & Haynes, M. P. 1995, *ApJ*, 444, 41
- Struble, M. F. & Rood, H. J. 1991, *ApJS*, 77, 363
- Tonry, J. L., Blakeslee, J. P., Ajhar, E. A., & Dressler, A. 1997, *ApJ*, 475, 399
- West, M. J., Côté, P., Jones, C., Forman, W., & Marzke, R. O. 1995, *ApJ*, 453, L77
- Whitmore, B. C. et al. 1995, *ApJ*, 454, L73
- Wing, D. L., Harris, G. L. H., Hanes, D. A., & Harris, W. E. 1995, *AJ*, 109, 121
- Zabludoff, A. I., Geller, M. J., Huchra, J. P., & Ramella, M. 1993, *AJ*, 106, 1273

Table 1. Metric Specific Frequencies for Sample Galaxies

Galaxy	$S_N$ $^{+}_{-}$	Galaxy	$S_N$ $^{+}_{-}$	Galaxy	$S_N$ $^{+}_{-}$
A262-1	5.0 $^{1.5}_{1.3}$	A999-1	3.9 $^{1.5}_{1.3}$	A1656-3	4.6 $^{1.5}_{1.3}$
A347-1	5.8 $^{1.6}_{1.3}$	A1016-1	3.3 $^{1.2}_{1.1}$	A2162-1	7.4 $^{2.2}_{1.8}$
A397-1	4.7 $^{1.4}_{1.1}$	A1177-1	4.2 $^{1.3}_{1.0}$	A2197-1	2.5 $^{1.4}_{1.3}$
A539-1	9.1 $^{3.0}_{2.6}$	A1185-1	6.4 $^{1.8}_{1.4}$	A2197-2	5.9 $^{1.5}_{1.2}$
A539-2	9.4 $^{3.0}_{2.4}$	A1314-1	4.2 $^{1.1}_{1.0}$	A2199-1	8.1 $^{2.3}_{1.9}$
A569-1	3.0 $^{1.2}_{1.0}$	A1367-1	5.3 $^{1.4}_{1.1}$	A2634-1	7.5 $^{2.1}_{1.7}$
A634-1	4.0 $^{1.2}_{1.0}$	A1656-1	5.7 $^{1.3}_{1.3}$	A2666-1	3.5 $^{1.1}_{1.0}$
A779-1	4.1 $^{1.0}_{0.9}$	A1656-2	9.3 $^{2.0}_{2.0}$		

Note. —  $S_N$  values are calculated within  $32 h^{-1}$  kpc of the center of each galaxy assuming the M87 GCLF shifted according to the cluster CMB frame velocity; a CMB velocity of  $1310 \text{ km s}^{-1}$  has been adopted for Virgo.

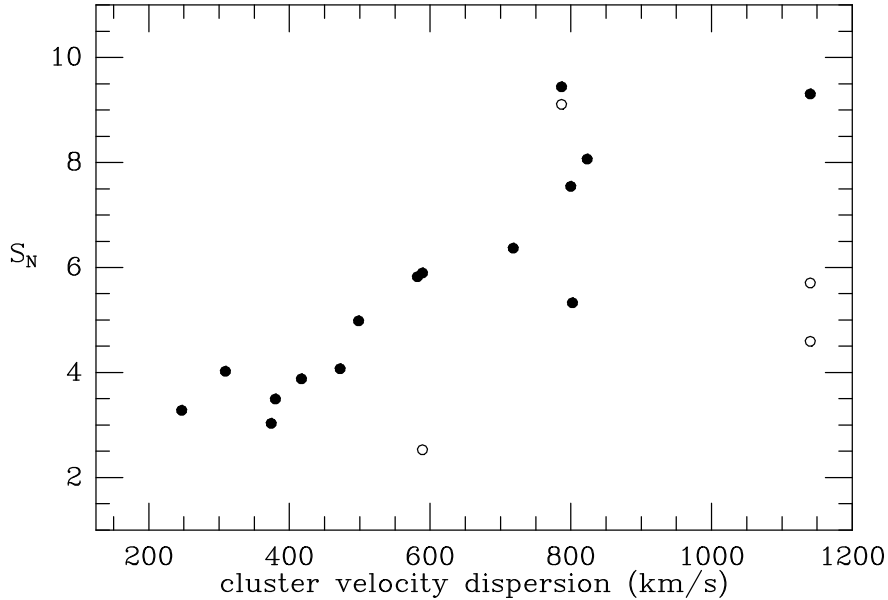


Fig. 1.— The derived  $S_N$  values are shown plotted against cluster velocity dispersion, collected from the literature, within one Abell radius of the cluster center. Filled circles represent the central bright galaxies in the clusters; open circles represent less central galaxies for clusters with more than one member in the sample (see text for details).



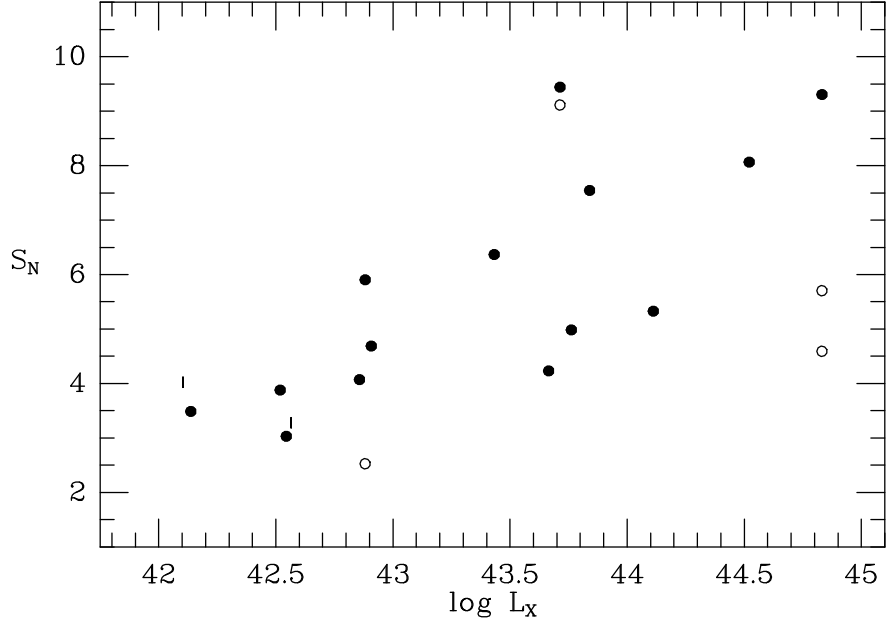


Fig. 2.—  $S_N$  is plotted against the total X-ray luminosity ( $\text{ergs sec}^{-1}$ ) within  $0.5 h^{-1} \text{Mpc}$  of the cluster X-ray center. The two short vertical lines represent upper limits on the X-ray luminosity; otherwise, symbols are as in Figure 1.

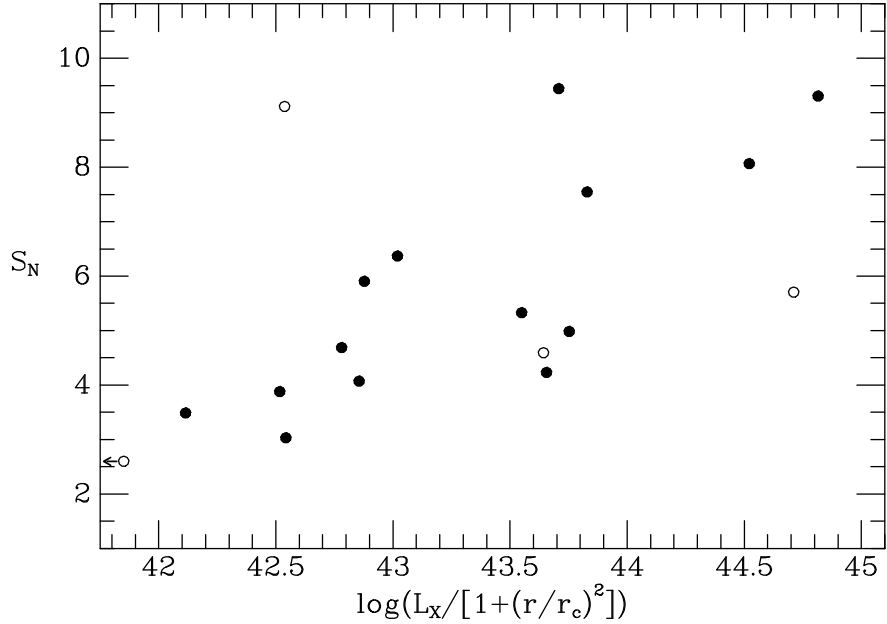


Fig. 3.—  $S_N$  is plotted against the radially weighted, or “local”, X-ray luminosity at the galaxy position within the cluster. The correlation observed in Figure 3 improves slightly with this weighting. The point for A2197-1, shown with an arrow, would be located at  $\log[L_X/(1+r^2/r_c^2)] = 40.8$ .

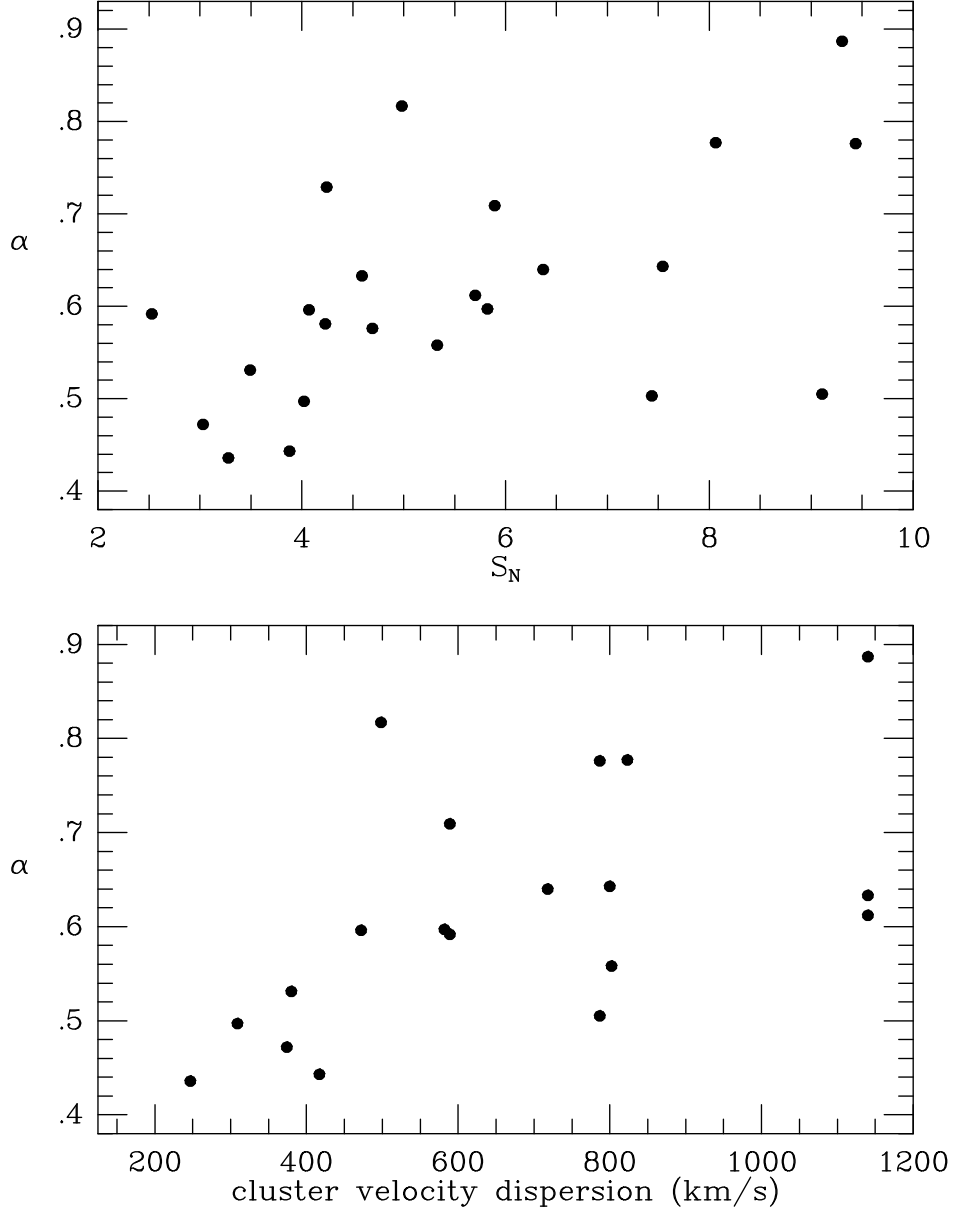


Fig. 4.— The profile structure parameter  $\alpha$ , a measure of galaxy extent, is plotted against  $S_N$  (top) and cluster velocity dispersion (bottom). The correlation between  $S_N$  and  $\alpha$  appears to be a consequence of the fact that both are dependent on cluster density, reflected by the velocity dispersion.